Eur. J. Mineral.
2006, **18**, 753–764

Interpretation of the nontronite-dehydroxylate Mössbauer spectrum using EFG calculations

LIDIA G. DAINYAK[1,*], BELLA B. ZVIAGINA[1], VIACHESLAV S. RUSAKOV[2] and VICTOR A. DRITS[1]

[1]Geological Institute of the Russian Academy of Science, Pyjzhevsky Street 7, 119017 Moscow, Russia
[*]Corresponding author, e-mail: dainyak@ginras.ru
[2]Moscow State University, Department of Physics, Vorobyovy Gory, 119899, Moscow, Russia

Abstract: Dehydroxylated Garfield nontronite has been studied using Mössbauer spectroscopy. According to literature, in dehydroxylated Fe^{3+}-rich dioctahedral 2:1 phyllosilicates (celadonites, glauconites and nontronites), the octahedral cations migrate from *cis*- into *trans*-sites with the formation of five-fold coordination of the former *cis*- and *trans*-octahedra. Therefore, the two main fitted doublets with quadrupole splittings, Δ, of 0.906 and 1.392 mm/s are supposed to be related to Fe^{3+} in the former *cis*- and *trans*-octahedra. To assign these doublets to this or that positions, analysis of Pauling's bond strength (PBS), structural modeling and EFG calculations were performed. The calculated quadrupole splittings for Fe^{3+} located in the former *cis*- and *trans*-octahedra in the nontronite-dehydroxylate structure are equal to 1.295 and 1.026 mm/s, respectively. On the basis of the calculation results, the quadrupole doublet with smaller Δ should be assigned to the former *trans*-octahedra whereas the doublet with larger Δ should be assigned to the former *cis*-octahedra.

The calculated EFG parameters proved to be independent of the mode in the layer stacking, which confirms the major role of the Fe^{3+} nearest environment in the formation of the different EFGs at Fe nuclei.

Possible disruptions of two-dimensional continuity of dehydroxylated octahedral sheets that may be a reason for superparamagnetic effects in nontronite-dehydroxylates at low temperatures are discussed in terms of the structural model of dehydroxylated Fe-rich dioctahedral 2:1 phyllosilicates.

Key-words: Mössbauer spectroscopy, EFG calculations, nontronite-dehydroxylate, structural modelling.

1. Introduction

Nontronite is a dioctahedral layer silicate having an idealized crystal-chemical formula $A_x[Si_{4-x}Al_x]Fe_2^{3+}O_{10}(OH)_2 \cdot n\ H_2O$, where A represents the interlayer cation. Its structure consists of 2:1 layers separated by water molecules and exchangeable cations. Each 2:1 layer is formed by edge sharing octahedra sandwiched between sheets of corner sharing (Si, Al) tetrahedra. A 2:1 layer unit cell contains three symmetrically independent octahedra, one *trans*- and two *cis*-octahedra, which differ in the arrangement of hydroxyl groups. Adjacent *cis*-octahedra share an edge formed by two OH groups whereas in *trans*-octahedra hydroxyls are located opposite each other. The *trans*-octahedral site is denoted as M1 and two *cis*-sites as M2 and M2'. X-ray and electron diffraction studies showed that in nontronite *trans*-octahedra are vacant and octahedral cations are located only in M2 and M2' sites (Besson *et al*., 1982, 1983; Bonnin *et al*., 1985; Tsipursky & Drits, 1984; Tsipursky *et al*., 1978, 1985a; Manceau *et al*., 2000).

Structural refinements of thermally transformed dioctahedral phyllosilicates were first made for Al-rich *trans*-vacant (*tv*) varieties, such as pyrophyllite-1Tc (Wardle & Brindley, 1972) and muscovite (Udagava *et al*., 1974). In a *tv* Al-rich dehydroxylated octahedral sheet, the two adjacent hydroxyls are replaced by a residual oxygen, O_r, having the same *z* coordinate as the octahedral cation, and Al cations have a five-fold coordination. Drits *et al*. (1995) noted that disposition of O_r in the octahedral cation plane of octahedral Al cations leads to appropriate Al-O_r bond lengths providing stability of a *tv* dehydroxylated structure. That is, Al cations have no reason to migrate in course of thermally induced transformations of octahedral 2:1 sheets.

Tsipursky *et al*. (1985b) using oblique texture electron diffraction showed that in dehydroxylated Fe^{3+}-rich dioctahedral 2:1 phyllosilicates (celadonites, glauconites and nontronites) the octahedral cations migrate from *cis*- into *trans*-octahedra. Later, Muller *et al.* (1998, 2000) determined the actual structure of two dehydroxylated Fe-rich dioctahedral 2:1 layer silicates by comparison of the experimental XRD patterns with those calculated for structural models acceptable from crystal-chemical point of view. In Fe-rich dehydroxylated dioctahedral phyllosilicates, unlike Al-rich varieties, the residual oxygens are located not in the plane of octahedral cations but in one of the two adjacent former OH positions providing five fold coordination of each cation in the dehydroxylated octahedral sheet. Migration of Fe^{3+} cat-

DOI: 10.1127/0935-1221/2006/0018-0753
0935-1221/06/0018-0753 $ 5.40

ions into former *trans*-octahedra and location of O_r in the former OH sites ensure appropriate Fe-O_r bond lengths and stabilize the dehydroxylated structure.

Dehydroxylated 2:1 dioctahedral phyllosilicates (montmorillonites, nontronite, celadonites, muscovites) were studied using Mössbauer spectroscopy by Heller-Kallai & Rozenson (1980). These authors erroneously supposed that in nontronite Fe^{3+} cations occupy M1 and M2 positions, that is, that nontronite is *cis*-vacant. In addition, by analogy with dehydroxylated Al-rich dioctahedral 2:1 phyllosilicates (Wardle & Brindley, 1972), they speculated that there was no migration of Fe^{3+} in course of dehydroxylation process. This resulted in a rather confused interpretation of the two quadrupole doublets fitted to the nontronite SWa-1 dehydroxylate spectrum. The inner doublet was assigned to Fe^{3+} in 5-coordinated M2 position whereas the outer one was assigned to Fe^{3+} in a very distorted 6-coordinated M1 position.

Karakassides *et al*. (2000) investigated Mössbauer spectra of dehydroxylated nontronite SWa-1 measured in the temperature interval of 1.95–80K and revealed superparamagnetic behavior with a blocking temperature of ~5K. The paramagnetic component of the spectrum is fitted with two quadrupole doublets. The isomer shifts and quadrupole splittings agree well with those reported by Heller-Kallai & Rozenson (1980). Basing on X-ray and electron diffraction data, according to which the *trans*-positions of the nontronite structure are vacant (Méring & Oberlin, 1967; Besson *et al*., 1982; Sakharov *et al*., 1990; Tsipursky & Drits, 1984; Tsipursky *et al.*, 1985a), and Fe^{3+} cations migrate into *trans*-positions in the course of dehydroxylation (Tsipursky *et al*., 1985b), these authors infer that heat-treated nontronites may show two Fe^{3+}-doublets, one related to Fe^{3+} in the former *cis*- and the other in the former *trans*-octahedra, both of them being five coordinated. However, inner and outer doublets were not assigned to this or that position.

Natural SWa-1 nontronite, like six other nontronites investigated by Lear & Stuki (1990), exhibits non-ideal antiferromagnetic exchange interactions at low temperature. There was no uniform model to explain this phenomenon. Lear & Stuki (1990) considered several reasons, such as magnetic dilution due to isomorphous substitutions by diamagnetic cations (Al, Mg) or antiferromagnetic frustration due to clustering of Fe^{3+} cations into triads, either within the octahedral sheet (implying no less than 13% occupancy of *trans*-sites) or between octahedral and tetrahedral sheets. Based on high-precision data of EXAFS, P-EXAFS spectroscopy and X-ray diffraction (Manceau *et al*., 2000), four reference nontronite samples including SWa-1 were shown to be *trans*-vacant within the detection limit of 5% of total iron. For SWa-1 nontronite, no detectable $^{IV}Fe^{3+}$ was found, and a structural model for the two-dimensional distribution of cations in the octahedral sheets was proposed. This model includes magnetic domains separated by diamagnetic cations, which is considered to be the most probable reason for the observed magnetic properties of SWa-1 nontronite.

To explain superparamagnetic effects in dehydroxilated SWa-1 nontronite, Karakassides *et al.* (2000) suggested the presence of small magnetic domains resulting from Fe-O-Fe bonds partially broken upon heat treatment. This explanation seems to be rather general and does not contain any crystal chemical or structural considerations.

The aim of the present study is to assign the Fe^{3+} doublets fitted to nontronite-dehydroxylate Mössbauer spectrum to five-fold former *cis*- and *trans*-octahedra using the analysis of Pauling's bond strength (PBS), structural modeling and EFG calculations. Possible disruptions of two-dimensional continuity of dehydroxylated octahedral sheets of nontronites are also discussed.

2. Experiment

The nontronite sample used in this study was from Garfield, Washington. The crystal-chemical formula $Na^{+}_{0.41}[Si_{3.61}Al_{0.39}](Fe^{3+}_{1.82}Al_{0.16}Mg_{0.02})O_{10}(OH)_2$ obtained by microprobe analysis coincides with the data of Manceau *et al*. (2000).

The natural nontronite powder was heated at 700° C for 6 h. The treatment conditions corresponded to those of Tsipursky *et al*. (1985b) and Muller *et al*. (1998) and the monomineral nontronite-dehydroxylate was identified by X-ray diffraction.

The room temperature Mössbauer spectrum was measured on a constant acceleration spectrometer using a Co^{57} (Rh) source (source half-width Γ = 0.107 mm/s) and calibrated with reference to α-Fe. The absorber was prepared in a hollow cone form with approximately 55° half-cone angle to eliminate orientation effects (Popov *et al.*, 1988). The amount of the sample was regulated to produce the Mössbauer effect value (MEV) that would belong to the region of a linear dependence of MEV on the absorber thickness. Thus the Mössbauer effect value of ~6% corresponds to the thin absorber condition. The statistics ensures the good quality of the spectrum with k= 210, where k is the maximum absorption divided by standard deviation (square root of number of counts per channel) (Rusakov, 2005). The spectrum measured within greater Doppler velocities interval confirmed the absence of a magnetic phase which could be formed during the heat-treatment of Garfield nontronite.

2.1 Refinement of the nontronite dehydroxylate spectrum

The spectrum was refined with the help of the program SPECTR from the complex MSTools (Rusakov, 2000; Rusakov & Chistyakova, 1992). At first, two doublets expected to correspond to former *cis*- and former *trans*-octahedra were fitted (variant 1) using a Lorentzian line shape. The equality of the amplitudes ($A_{-v} = A_{+v}$) and the half-widths ($\Gamma_{-v} = \Gamma_{+v}$) of the components belonging to each individual doublet was imposed as a restriction. Unacceptable χ^2 = 24.14, great systematic deviations (SD) between the envelope curve and the experimental spectrum, which is shown below each fitted spectrum in Fig. 1, and the big difference (35%) between the Γ_1 and Γ_2 values (Table 1) suggested that one more doublet should be added. The corresponding fitting (variant 2) did not lead to a radical improvement in the results. The fitting, as before, is characterized by very large χ^2 and SD values (Fig. 1, variant 2) and by even greater dif-

ference (up to 43%, Table 1) between Γ values. The comparable areas S under the doublet components disagree with the clear structural model that involves former *cis*- and *trans*-octahedra. The introduction of the additional Lorentzian line shape doublet(s) would improve the statistical characteristics of the fitting. However, it would also complicate the application of this model even to a greater extent.

The failure of the Lorentzian line shape fitting may imply the presence of a partial local inhomogeneity in the nontronite dehydroxylate structure. Under the assumption of the independent Gaussian distribution of isomer shifts, δ, and quadrupole splittings, Δ, resulting from the local inhomogeneity, a pseudo-Voigt line shape fitting is the most appropriate (Evans & Black, 1970; David, 1986; Martin & Puerta, 1981; Rancourt & Ping, 1991; Rusakov, 1999; Presniakov *et al.*, 2006). Several variants were analyzed. Variants 3 and 4 (Fig. 1) use the same constraints, such as $A_{-v} = A_{+v}$ and $\Gamma_{-v} = \Gamma_{+v}$, and include two and three doublets, respectively. The χ^2 and SD values decrease in comparison with Lorentzian line shape variants but still do not satisfy the statistical criteria of a spectrum refinement. Besides, the big difference between Γ values remains, up to 38% and 56% for variants 3 and 4, respectively (Table 1).

The next step accounts for a possible linear correlation between the changing δ and Δ values. In this case, the equality of the doublet areas, $S_{-v} = S_{+v}$, is imposed as the constraint whereas the half-widths of the doublet components, Γ_{-v} and Γ_{+v}, are released during the fitting process. Variants 5 and 6 conform to these conditions and include two and three doublets, respectively. In variant 5, despite the acceptable χ^2 and SD values (Fig. 1), significant differences between Γ_1 and Γ_2 values (up to 33%) and between Γ_{-v} and Γ_{+v} values (up to 16%) are observed (Table 1). The introduction of the third doublet into the fitting procedure (variant 6) not only leads to the good statistical characteristics of the spectrum refinement but also decreases the difference between Γ values (down to a maximum of 19%) and Γ_{-v} and Γ_{+v} values (down to a maximum of 10%) (Table 1). Variant 6 is accepted as a reliable refinement of the nontronite dehydroxylate spectrum.

Note that the intermediate (1–5, Table 1) and the final fitting variants (6, Table 1) display similar relationships between subspectra S values ($S_1 < S_2$) and a relative invariability for the isomer shifts, δ.

3. Results

The fitted Mössbauer spectrum of the nontronite dehydroxylate is shown at Fig.1, variant 6. Table 1 gives the ^{57}Fe Mössbauer parameters. The doublets with quadrupole splittings, Δ, of 0.906 and 1.392 mm/s are supposed to be related to Fe^{3+} in the former *cis*- and *trans*-octahedra. These Δ values agree with the data of Heller-Kallai & Rozenson (1980) and Karakassides *et al*. (2000). The increase in Δ values in comparison with those for natural nontronite spectrum (Δ_1=0.25 mm/s, Δ_2=0.65 mm/s (Bonnin *et al.*, 1985), Δ_1=0.24 mm/s, Δ_2=0.66 mm/s (Sherman & Vergo, 1988)) reflects substantial deformation of Fe^{3+} polyhedra when coordination changes from six-fold to five-fold one. The Δ values of 2.212 mm/s for the outer doublet is abnormally high for Fe^{3+} and should be associated with unusual coordination.

The behavior of the isomer shift, δ, is rather surprising. One should expect the δ values to decrease with decreasing Fe^{3+}-coordination. However, the δ values for the basic doublets of the dehydroxylate spectrum (0.371 mm/s and 0.366 mm/s) are the same as the those for the spectrum of untreated Garfield nontronite ($\delta_1=\delta_2$=0.37 mm/s (Bonnin *et al.*, 1985) and $\delta_1=\delta_2$= 0.37 mm/s (Sherman &Vergo, 1988)). Similar results for SWa-1 nontronite-dehydroxylate were reported by Heller-Kallai & Rozenson (1980) and Karakassides *et al*. (2000). The δ value for the third doublet of the dehydroxylate spectrum (0.384 mm/s, Table 1) also corresponds to six-fold coordination of Fe^{3+}.

As mentioned in the previous section, the difference of about 10% between half-widths Γ_{-v} and Γ_{+v} implies the presence of the partial local inhomogeneity in the nontronite dehydroxylate structure. The nature of this inhomogeneity will be analyzed in detail in Sections 3.1 and 3.2.

3.1 Factors affecting the electric field gradient (EFG) at Fe^{3+} nuclei in the nontronite-dehydroxylate.

Crystal-chemical and structural peculiarities of 2:1 dioctahedral *trans*-vacant Fe-rich phyllosilicates make it possible to analyze the local structural inhomogeneity in terms of the local cation arrangements. In the case of ^{57}Fe Mössbauer spectroscopy, it is appropriate to place the Fe cation into the centre of such arrangements. The variety in the local cation environments in a mineral structure depends on its cation composition and cation distribution. In celadonites, glauconites, ferriillites and leucophyllites characterized by extensive isomorphism in the octahedral sheet (Fe^{3+}, Fe^{2+}, Al, Mg) the individual quadrupole doublets Fe^{3+} and Fe^{2+} are mainly determined by the nature of three octahedral cations nearest to Fe^{3+} and Fe^{2+} (Drits *et al.*, 1997; Dainyak *et al.*, 2004). The model refinements of Mössbauer spectra of these minerals confirmed that the composition of the local cationic arrangements is the principal factor affecting the EFG on Fe nuclei in micaceous dioctahedral minerals.

In the natural Garfield nontronite, because of the predominance of Fe^{3+} in octahedra, the local cation arrangements include the nearest tetrahedral cations. Goodman (1978) suggested that trivalent tetrahedral cations could cause a non-equivalent EFG at the *cis*-sites, and consequently more than one quadrupole doublet in the Mössbauer spectrum of untreated nontronite. Based on point-charge calculations, Dainyak & Drits (1987) confirmed this supposition and found that Δ for the arrangement $3Fe^{3+}$ around Fe^{3+} adjacent to four tetrahedral Si ([4Si](3Fe^{3+})) is about half of Δ for the arrangement [3SiAl](3Fe^{3+}). The statistical amount of the [3SiAl](3Fe^{3+}) arrangements in Garfield nontronite is about 30% with expected $S_{[3SiAl](3Fe^{3+})}/S_{[4Si](3Fe^{3+})}$ ratio of about 0.8. The areas under the fitted doublets satisfy this ratio (Goodman *et al.*, 1976; Dainyak & Drits, 1987). Thus the main factor affecting the EFG in untreated Garfield nontro-

Table 1. Mössbauer parameters for the Garfield nontronite dehydroxylate spectrum corresponding to the different refinement variants. Variant 6 with $\chi^2 = 1.07$ is accepted as the final one.

							Fitting conditions	
Variant	Fe^{3+} doublet	δ (mm/s)	Δ (mm/s)	Γ_{-v} (mm/s)	Γ_{+v} (mm/s)	S (%)	Line shape	Constraints
1	1	0.379±0.005	0.960±0.010	0.375±0.020	0.375±0.020	37.8±0.3	Lorentzian	$A_{-v} = A_{+v}$
	2	0.370±0.015	1.488±0.029	0.576±0.020	0.576±0.020	62.2±0.4		$\Gamma_{-v} = \Gamma_{+v}$
2	1	0.373±0.010	0.812±0.019	0.308±0.025	0.308±0.025	22.9±0.6	Lorentzian	$A_{-v} = A_{+v}$
	2	0.379±0.010	1.230±0.019	0.390±0.044	0.390±0.044	43.5±1.2		$\Gamma_{-v} = \Gamma_{+v}$
	3	0.356±0.020	1.748±0.038	0.544±0.022	0.544±0.022	33.6±0.7		
3	1	0.383±0.004	1.034±0.007	0.514±0.011	0.514±0.011	41.3±0.7	Pseudo-Voigt	$A_{-v} = A_{+v}$
	2	0.363±0.013	1.492±0.026	0.835±0.013	0.835±0.013	58.7±0.8		$\Gamma_{-v} = \Gamma_{+v}$
4	1	0.382±0.008	1.024±0.016	0.534±0.026	0.534±0.026	47.5±2.7	Pseudo-Voigt	$A_{-v} = A_{+v}$
	2	0.365±0.045	1.514±0.090	0.765±0.068	0.765±0.068	50.8±2.9		$\Gamma_{-v} = \Gamma_{+v}$
	3	0.455±0.024	2.426±0.048	0.334±0.097	0.334±0.097	1.7±1.4		
5	1	0.393±0.004	1.050±0.008	0.535±0.009	0.574±0.011	57.9±1.4	Pseudo-Voigt	$S_{-v} = S_{+v}$
	2	0.336±0.028	1.656±0.057	0.724±0.026	0.861±0.034	42.1±1.5		$\Gamma_{-v} \neq \Gamma_{+v}$
6	1	0.371±0.008	0.906±0.016	0.467±0.012	0.519±0.016	39.1±2.5	Pseudo-Voigt	$S_{-v} = S_{+v}$
	2	0.366±0.012	1.392±0.024	0.576±0.033	0.537±0.033	49.7±2.8		$\Gamma_{-v} \neq \Gamma_{+v}$
	3	0.384±0.022	2.212±0.044	0.483±0.021	0.531±0.025	11.2±1.0		

nite is the Al for Si substitution in the tetrahedral sheets whereas the local variations in octahedral cation arrangements around Fe^{3+} ($2Fe^{3+}Al$, $2AlFe^{3+}$, 3Al), which, statistically, do not exceed 25%, are supposed to broaden the doublet components.

The situation radically changes in Garfield nontronite-dehydroxylate. During thermally induced migration of Fe^{3+} cations from *cis*- into *trans*-octahedra, the unit cell transforms from the *C*-centered into a primitive one (Muller *et al*., 1998). Figure 2 shows the structural model of the dehydroxylated octahedral sheet of the 2:1 layer with symmetrically independent former *cis*- (M21, M22) and former *trans*-octahedra (M11, M12) and residual oxygens in the former OH group positions. The detailed description of this model is given in Muller *et al*. (1998, 2000). The residual oxygen in the former *cis*- or *trans*-octahedron, along with the other four oxygens, belong to the first coordination sphere of Fe^{3+}. Therefore, the presence of the former *cis*- and *trans*-octahedra should be supposed to be one of the main factors determining the EFG at Fe^{3+} nuclei. The local arrangements including the next neighbors, like in the untreated nontronite, also consist of three cations. However, as it follows from Fig. 2, now every Fe^{3+} cation in the former *cis*-octahedra (M21, M22) has three nearest neighboring cations in the former *trans*-octahedra whereas every Fe^{3+} cation in the former *trans*-octahedra (M11, M12) is surrounded by three adjacent cations in the former *cis*-octahedra. The local arrangements comprising Al cations both in tetrahedral and octahedral sheets should create their own EFG on Fe nuclei. Bearing in mind the above evaluations for their statistical amounts, the areas under the corresponding doublet components are expected to be minor with respect to those corresponding to M21, M22 and M11, M12 doublets. A qualitative relationship between the EFG affecting Fe nuclei in the different local arrangements can be derived from the Pauling's bond strengths analysis.

3.2 Pauling's bond strengths analysis

Pauling's bond strength (PBS) is calculated as the cation formal charge divided by the cation coordination number and is expressed in valency units (v.u.). In general, the sum of bond strengths received by an anion may differ from its formal charge. The corresponding values will be referred to as USPBS (uncompensated sum of Pauling's bond strengths).

Figure 3 shows schematically (upper row, *a*, from left to right) the Fe^{3+}-bearing polyhedra in the local arrangements [4Si]($3Fe^{3+}$) for the six-fold *cis*-position in the untreated nontronite structure and for the former *cis*- and *trans*-octahedra with five-fold coordination in the nontronite-dehydroxylate structure. The lower row (*b*) corresponds to the arrangements [3SiAl]($3Fe^{3+}$). As an example, only one of the four possible positions of an Al tetrahedron is shown. The USPBS values for O^{2-}, OH^- and O^{2-}_r are indicated near the corresponding positions.

The arrangement [4Si]($3Fe^{3+}$) in untreated nontronite is totally balanced as all individual USPBS values are equal to zero. Note that the arrangements of the [4Si]($2AlFe^{3+}$) type should be also balanced because Al and Fe^{3+} cations have the same charge. The transformation of six-fold into five-fold coordination in the course of dehydroxylation creates dramatic anisotropy in the individual USPBS distribution (Fig. 3). Four of the five apices in the polyhedra in the centre of the arrangement [4Si]($3Fe^{3+}$) are oversaturated while that corresponding to residual O^{2-}_r is strongly undersaturated with respect to the positive charge (Fig. 3, row *a*). The Mössbauer spectrum of the nontronite-dehydroxylate reflects this anisotropy as increasing quadrupole splittings. The former trans-octahedron whose residual O^{2-}_r is at the pinnacle of the pyramid, looks more symmetrical in comparison with the former *cis*-octahedron, where the residual O^{2-}_r is located at the pyramid base. Accordingly, the EFG at Fe^{3+} nuclei located in the former *cis*-octahedra may be expected to be

greater than the one at Fe^{3+} nuclei located in the former *trans*-octahedra.

The Al-substituted tetrahedron adjacent to Fe^{3+} in the arrangement [3SiAl]($3Fe^{3+}$) adds to the asymmetry in the distribution of the USPBS values. However, these changes are of a second rank with respect to the changes associated with the formation of the former *cis*- and *trans*-octahedra during dehydroxylation (Fig. 3, row *a*). For the arrangement [3Si-Al]($3Fe^{3+}$), one may expect a slightly smoothed asymmetry of former *cis*-octahedra and slightly increased asymmetry of former *trans*-octahedra in comparison with that for the arrangements [4Si]($3Fe^{3+}$). Here again, the arrangements comprising the octahedral Al bring nothing new into the distribution of the USPBS values.

The above considerations imply the Fe^{3+} nearest surroundings differing in the positions of the residual oxygens to be the main factor affecting the EFG on Fe nuclei in the nontronite dehydroxylate structure. To confirm this supposition, the modeling of its structure and EFG calculations were performed.

3.3 Modeling of Garfield nontronite-dehydroxylate structure

The structures of both initial untreated Garfield nontronite and its dehydroxylate have a very low degree of structural ordering**.** However, the previous studies on the cation distribution in *trans*-vacant dioctahedral micaceous minerals based on the assignment of the individual quadrupole doublets Fe^{3+} and Fe^{2+} to the local cationic arrangements (Drits *et al*., 1997; Dainyak *et al*., 2004), showed that it is the nearest environment of the Fe nuclei that is the main factor affecting the EFG. Therefore the mode in the layer stacking should have little or no effect on the results of EFG calculations. On the other hand the algorithm for the EFG calculations can be used only for periodic crystal structures. Therefore the EFG calculations for Garfield nontronite dehydroxylate are made in terms of a strictly periodic structural model. To confirm the weak influence of the mode in the layer stacking, the EFG parameters were calculated for two models of the nontronite dehydroxylate having the same

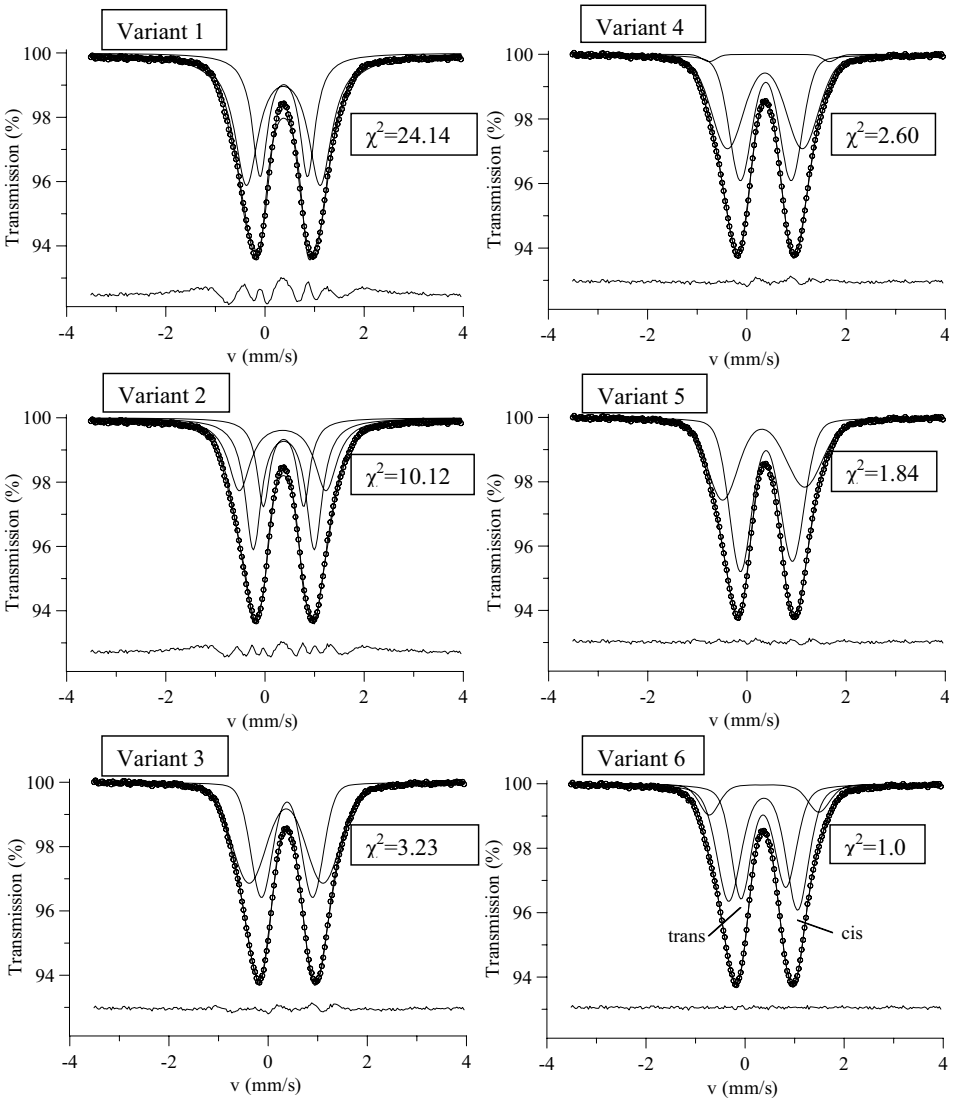

Fig. 1. Variants for the refinement of the Mössbauer spectrum (RT) of Garfield nontronite dehydroxylate.

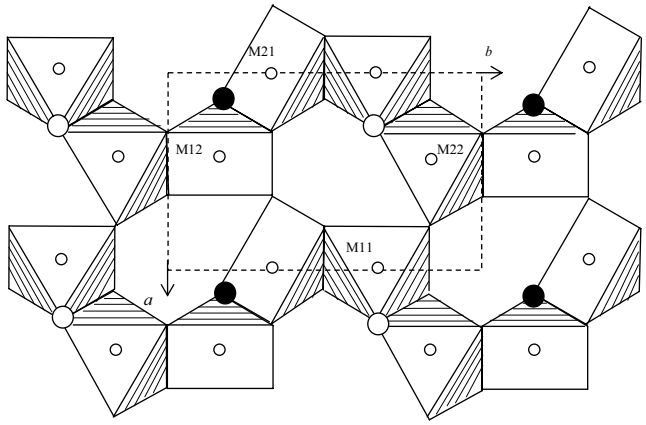

○- Fe cations; ◯ - Upper residual oxygen; ● - Lower residual oxygen

Fig. 2. Dehydroxylated primitive unit-cell (dashed line) in a structural model of the octahedral sheet with the former *cis*- (M21, M22) and *trans*-octahedra (M11, M12). Residual oxygens, O^{2-}_{r}, alternate between positions above and below the plane of octahedral cations (by Muller *et al*., 2000).

structure of the layer: one with monoclinic layer stacking and the other with orthogonal layer stacking.

Besson *et al.* (1983) and Tsipursky & Drits (1984) showed, using oblique-texture electron diffraction, that K-saturation and subjection to numerous wetting-and-drying cycles according to the technique of Mamy & Gaultier (1976) improves the structural ordering of Garfield nontronite, so that it can be described in terms of a one-layer monoclinic unit cell. Based on the data of Besson *et al.* (1983) and Tsipursky & Drits (1984), Manceau *et al.* (1998) provided the following unit-cell parameters for the Na-exchanged Garfield nontronite: a = 5.277 Å, b = 9.140 Å, c = 9.780 Å, β = 101.0° (space group *C2/m*). This unit cell and the crystal chemical formula are used to determine the nontronite-dehydroxylate structural models according to the following procedure. At the first stage, the atomic coordinates in the layer unit cell for a *tv* nontronite structure for all symmetrically independent atoms except interlayer Na were calculated using the algorithm of Smoliar-Zviagina (1993), which is based on regression equations relating structural parameters and chemical composition of micaceous minerals that were obtained from the analysis of structural refinements of micas of various compositions published in the literature. The same algorithm was used to calculate the atomic coordinates of *tv* and *cv* 2:1 dioctahedral clay mineral structures (Manceau *et al*., 2000; Muller *et al*., 1998, 2000; Gates *et al*., 2002; Drits *et al*., 2006).

Table 2a. The simulated Cartesian atomic coordinates of the *tv* Garfield nontronite structure (a = 5.277 Å, b = 9.140 Å, *csin* β = 9.600 Å) and octahedral and tetrahedral cation-oxygen distances (Å).

	x	y	z
M	0.5	0.1667	0
T	0.3101	0.3291	0.2841
O1	0.3094	0.3122	0.1148
O2	0.3094	0.5	0.3293
O3	0.0593	0.75	0.348
OH	0.3741	0	0.1075
M – O1	1.999	T-O1	1.632
M – O1'	1.979	T-O2	1.623
M – OH	1.956	T-O3	1.623
mean	1.978	T-O3'	1.628
		mean	1.626

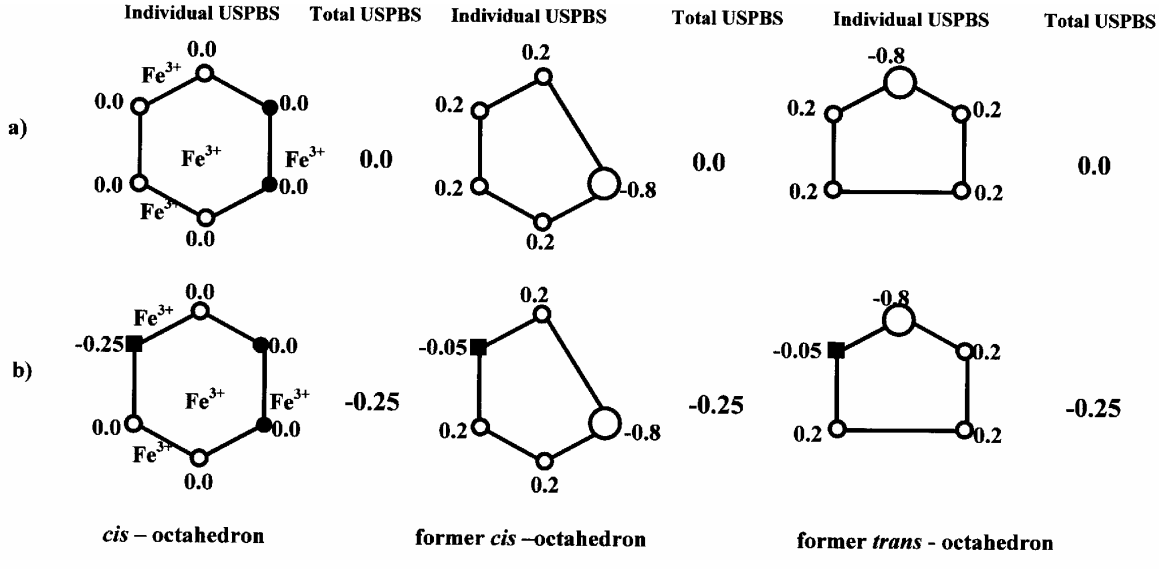

○- O^{2-}, shared by Si-tetrahedra; ■- O^{2-}, shared by Al-tetrahedra; ● - OH^- ; ◯ - residual O^{2-}

Fig. 3. Schemes of Fe^{3+}-bearing polyhedra in the local arrangement [4Si](3Fe^{3+}) (a) and [3SiAl](3Fe^{3+}) (b) for the six-fold *cis*-position and for the five-fold former *cis*- and *trans*-positions (from left to right). The USPBS values for O^{2-}, OH^- and O^{2-}_{r} are indicated near corresponding positions. Pauling's bond strengths: 3/4 and 4/4=1 for Al^{IV} and Si, respectively; 3/6 = 1/2 and 3/5 for Fe^{3+}, Al in six-fold and five-fold coordination, respectively.

Table 2b. The simulated Cartesian atomic coordinates of the Garfield nontronite dehydroxylate structure and selected cation-oxygen distances (Å). (Model 1: a = 5.277 Å, b = 9.140 Å, c = 9.750 Å, α = 90°, β = 100.07 °, γ = 90°. space group $P1$; model 2: a = 5.277 Å, b = 9.140 Å, c = 9.60 Å, α = 90°, β = 90°, γ = 90°, space group $P1$).

	x	y	z		
M11	0	0.667	0	M11-O12	1.943
M12	0.5	0.167	0	M11-O22	1.918
M21	0	0.333	0	M11-O32	1.943
M22	0.5	0.833	0	M11-O42	1.918
O11	0.380	–0.001	0.105	M11-OR1	1.923
O12	0.880	0.499	0.105	mean	1.929
O21	0.317	0.311	0.105		
O22	0.817	0.811	0.105	M12-O11	1.943
O31	0.620	–0.001	–0.105	M12-O21	1.918
O32	0.120	0.499	–0.105	M12-O31	1.943
O41	0.683	0.311	–0.105	M12-O41	1.918
O42	0.183	0.811	–0.105	M12-OR2	1.923
OR1*	0.3165	0.687	0.0975	mean	1.929
OR2*	0.183	0.187	–0.0975		
T11	0.351	–0.009	0.284	M21-O12	1.928
T12	0.851	0.491	0.284	M21-O21	1.964
T21	0.338	0.32	0.284	M21-O32	1.928
T22	0.838	0.82	0.284	M21-O41	1.964
T31	0.649	–0.009	–0.284	M21-OR2	1.896
T32	0.149	0.491	–0.284	mean	1.936
T41	0.662	0.32	–0.284		
T42	0.162	0.82	–0.284	M22-O11	1.928
O51	0.096	0.905	0.329	M22-O22	1.964
O52	0.596	0.405	0.329	M22-O31	1.928
O61	0.846	0.655	0.348	M22-O42	1.964
O62	0.346	0.155	0.348	M22-OR1	1.896
O71	0.595	0.905	0.348	mean	1.936
O72	0.095	0.405	0.348		
O81	0.904	0.905	–0.329		
O82	0.404	0.405	–0.329	Na-O52	2.668
O91	0.154	0.655	–0.348	Na-O61	2.646
O92	0.654	0.155	–0.348	Na-O71	2.645
O101	0.405	0.905	–0.348	Na-O51	2.667
O102	0.905	0.405	–0.348	Na-O61'	2.647
Na1**	0.845	0.155	0.37	Na-O72	2.649
Na2	0.345	0.655	0.37	mean	2.655
Na3	0.155	0.155	–0.37		
Na4	0.655	0.655	0.63		

* residual oxygens in the former OH sites

** the occupancy of each Na site is 0.41/2

The atomic coordinates of the untreated Garfield nontronite as well as the cation-oxygen bond lengths in the octahedral and tetrahedral sheets are given in Table 2a. The structural details such as cation-oxygen distances, tetrahedral tilt, octahedral flattening and counter-rotation of octahedral bases are in agreement with those published in the literature for Fe-bearing dioctahedral phyllosilicates (Bailey, 1984). Specifically, the $(M\text{-}O)_{mean}$ (1.978 Å) and M-OH (1.956 Å) distances appear more correct than the corresponding values of Manceau *et al.* (1998), who used the DVLS procedure to simulate the Garfield nontronite structure: $(M\text{-}O)_{mean}$ = 2.014 Å, which is too large, and M-OH = 2.03 Å, which should be shorter than M-O, according to numerous published structural data. In their further work, Manceau *et al.* (2000) used the algorithm of Smoliar-Zviagina (1993). The T-O distances (Table 2a) are in agreement with the published structural data on dioctahedral 2:1 phyllosilicates having similar composition of tetrahedral cations.

At the second stage, to obtain a *cv* structure, the fractional orthogonal coordinates of the upper half of the *tv*-layer (Table 2a) are rotated around c^* through –120° with respect to the original system of axes (Tsipursky & Drits, 1984). The atomic coordinates of the lower half-layer were then obtained with the help of a two-fold rotation axis parallel to b. As a result, the Cartesian fractional atomic coordinates for the *cv*-layer unit cell are obtained. Two of the four OH groups present in the unit cell were removed and the residual oxygens were placed in the other two former OH sites, as described by Muller *et al*. (2000), to produce an asymmetric unit cell. As the resulting average Fe-O distances of 1.98 Å seemed unrealistically large for a 5-coordination polyhedron, the former octahedral sheet was flattened by an additional 0.192 Å (i.e. 0.02 fractional units along z^*) to produce mean Fe-O bond lengths of about 1.93 Å, which is intermediate between Fe-O in tetrahedral and octahedral coordination (1.85–1.91 Å and 1.98 Å, respectively (Semenova *et al.*, 1977; Smoliar-Zviagina, 1993; Brigatti & Guggenheim, 2002; Gates *et al.*, 2002). As shown by Manceau *et al.* (2000), in order to provide good fit between the experimental and simulated XRD patterns of Garfield nontronite, the interlayer Na cation in the structural model should be shifted from the interlayer mid-plane by about 1Å to the surface of the basal oxygens of the tetrahedral sheet, so that realistic Na-O distances are obtained. To ensure Na-O distances of about 2.65 Å (Lin & Bailey, 1984) the sites of Na were placed at z = 0.37 and –0.37 (above and below the tetrahedral sheets), so that the interlayer cations project onto the centers of the hexagonal rings of basal tetrahedral oxygens, the occupancy of each of the four interlayer sites being 0.41/2 atoms per $O_{10}(OH)_2$.

The resulting Cartesian atomic coordinates of the unit cell of the dehydroxylated *cv* layer as well as selected interatomic distances, are given in Table 2b. In the first structural model the successive layers are shifted with respect to each other along the a axis by $-0.323a$ so that in the projection on the *ab* plane centers of ditrigonal rings of the upper tetrahedral sheet of the lower layer and of the lower sheet of the upper layer coincide. As a result a periodic structure with the cell parameters a = 5.277 Å, b = 9.140 Å, c = 9.750 Å, α = 90°, β = 100.07 °, γ = 90° (space group $P1$) is obtained. In the second structural model the layers are stacked without displacement, so that in the projection on the *ab* plane centers of ditrigonal rings of the upper tetrahedral sheet of the lower layer are shifted with respect to those of the lower sheet of the upper layer along the a axis by $0.323a$. The unit cell parameters for this periodic structure are a = 5.277 Å, b = 9.140 Å, c = 9.60 Å, α = 90°, β = 90 °, γ = 90°.

3.4 EFG calculations

In a point charge model, the EFG tensor at the position of the Fe^{3+} nuclei is expressed as (Ingalls, 1964) $V = (1 - \gamma_\delta) \cdot V_{lat}$ where γ_δ is the antishielding factor (Sternheimer, 1963) and

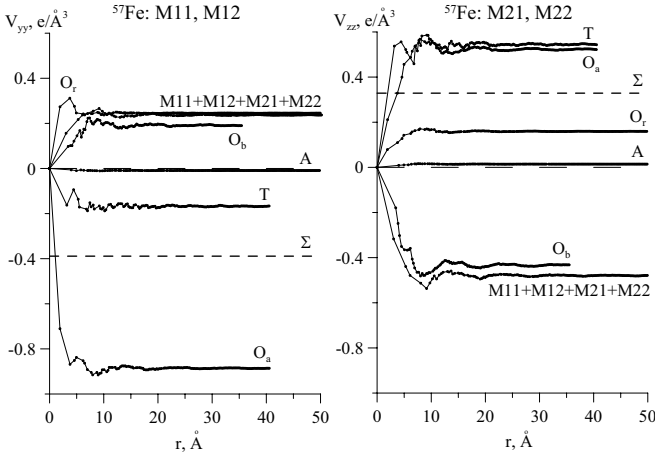

Fig. 4. The greatest component of the EFG tensor (before its diagonalization) at the Fe^{3+} nuclei in *cis*- (M21+M22) and *trans*-octahedra (M11+M12) resulting from all ions (Σ) and ions in distinct positions (O_a, O_b, O_r, T, A, M11+M12+M21+M22) of the nontronite dehydroxylate structure within the sphere with radius *r*.

V_{lat} is the EFG tensor resulting from the lattice point charges. For our nontronite-dehydroxilate structure, program LATTICE from complex MSTools (Rusakov, 2000; Rusakov & Chistyakova, 1992) calculates tensor V_{lat} as:

$V_{lat} = \Sigma_t V(t) = V(M11) + V(M12) + V(M21) + V(M22) + V(T) + V(O_a) + V(O_b) + V(O_r) + V(A)$.

Here $V(t) = e_t D(t)$ is a EFG tensor for atoms with the charge e_t in positions *t*, $D(t)$ is a matrix of the lattice sums for positions *t*. Each of the cation point charges e_{M11}, e_{M12}, and e_{M21}, e_{M22} at the former *trans*- and *cis*-positions, respectively, were assumed equal to +3 v.u.; the averaged charge of a tetrahedral cation, e_T, is equal to $3.61/4 \cdot 4 + 0.39/4 \cdot 3 = 3.90$ v.u.; the charges of basal (e_{O_b}), apical (e_{O_a}) and residual (e_{O_r}) oxygen anions are all equal to –2 v.u.; and the charge of the interlayer cation, e_A , is equal to 0.205 v.u. The component $D_{ij}(t)$ (Cartesian axis system is used for calculations) may be written as $D_{ij}(t) = \sum_{k(t)} \frac{3x^i_{k(t)} x^j_{k(t)} - \delta_{ij} r^2_{k(t)}}{r^5_{k(t)}}$, where δ_{ij} equals to 1 for $i = j$ and 0 for $i \neq j$, and $x_{k(t)}{}^i$ is the component ($i = x,y,z$) of the radius vector $\vec{r}_{k(t)}$ from the point of observation to the ion *k* having charge e_t. Calculation of the $D_{ij}(t)$ values was performed using the atomic coordinates of the nontronite-dehydroxylate given in Table 2b (model 1). The $V_{ij}(t)$ values are then calculated for each *t* atom and summed. The resulting tensor is then diagonalized to give the principal values of the EFG tensor.

The program takes account of $5 \cdot 10^3$ of each *t*-type atoms inside the sphere with the radius of over 36 Å (see Fig.4). Fig. 4 shows the greatest component of the EFG tensor (before its diagonalization) at the Fe^{3+} nuclei in *cis*- (M21+M22) and *trans*- (M11+M12) positions resulting from all ions (Σ) and ions in distinct positions (O_a, O_b, O_r, T, A, M11+M12+M21+M22) of the nontronite-dehydroxylate structure within the sphere with the radius *r*. It follows from Fig. 4 that the number of all the atoms ($\sim 45 \cdot 10^3$) included in the computation is sufficient to calculate V_{lat} within the accuracy of a few percent.

For each Fe^{3+} position, competitive contributions from different types of atoms are observed. The contribution of the interlayer cations (position A) is very small. Interestingly, the contributions from atoms of the same type except O_r, as well as the total contribution (Σ) have reverse signs for the former *cis*- and *trans*-sites.

Table 3. Quadrupole splittings, Δ, for symmetrically independent positions of Fe^{3+} in the nontronite dehydroxylate structure with the corresponding asymmetry parameters, η, and quadrupole coupling constants, e^2qQ. The last row shows the experimental Δ values.

Position	M11	M12	M21	M22
Calculated parameters				
Δ (mm/s)	1.026	1.026	1.295	1.295
η	0.815	0.815	0.726	0.726
e^2qQ	1.857	1.857	2.388	2.388
Experimental Δ (mm/s)	0.906		1.392	

When the EFG tensor is diagonalized, quadrupole splitting, $\Delta = \frac{1}{2} eQV_{zz} \left(1 + \frac{\eta^2}{3}\right)^{1/2} = \frac{e^2 qQ}{2} \left(1 + \frac{\eta^2}{3}\right)^{1/2}$ and asymmetry parameter, $\eta = (V_{xx} - V_{yy})/V_{zz}$, are calculated using the value of –9.1 for γ_8, and of 0.14 b(arn) for the nuclear quadrupole moment, Q (Rusakov & Khramov, 1992).

Table 3 shows the calculated quadrupole splittings, Δ, for symmetrically independent positions M11, M12, and M21, M22 in the nontronite-dehydroxylate structure with the corresponding asymmetry parameters, η, and quadrupole coupling constants, e^2qQ. Both former *trans*-octahedra (M11, M12) yield identical sets of the calculated parameters, and so do both former *cis*-octahedra (M21, M22). This is an additional confirmation of the correctness of the EFG calculation program. The EFG calculations made for the structural model with orthogonal layer stacking (model 2, Table 2b) reproduce the calculated parameters of Table 3 with the accuracy of 0.05% or better.

The calculated Δ values agree well with the experimental ones for two main doublets fitted to the Mössbauer spectrum of the nontronite-dehydroxylate (Table 3, last row). Based on the calculated results one may infer that the partial quadrupole doublet with smaller Δ should be assigned to the former *trans*-octahedra whereas the partial doublet with larger Δ should be assigned to the former *cis*-octahedra.

4. Discussion

Good agreement between calculated and experimental Δ values, which has ensured the assignment of the two main doublets fitted to the nontronite dehydroxylate spectrum, implies that at least two of the constituents involved in EFG calculations have contributed equally well. First, the simple point charge model turned out to be adequate. Bearing in mind that the bonding in 2:1 layer silicates is not purely ionic, it would seem appropriate to use effective charges instead of ionic charges. If, however, the effective charges are proportional to ionic charges with about the same or similar coefficients for all kinds of atoms, the calculations may be carried out in terms of the ionic point-charge model. The agreement between the calculated and experimental Δ values obtained using the nuclear quadrupole moment Q = 0.14 b

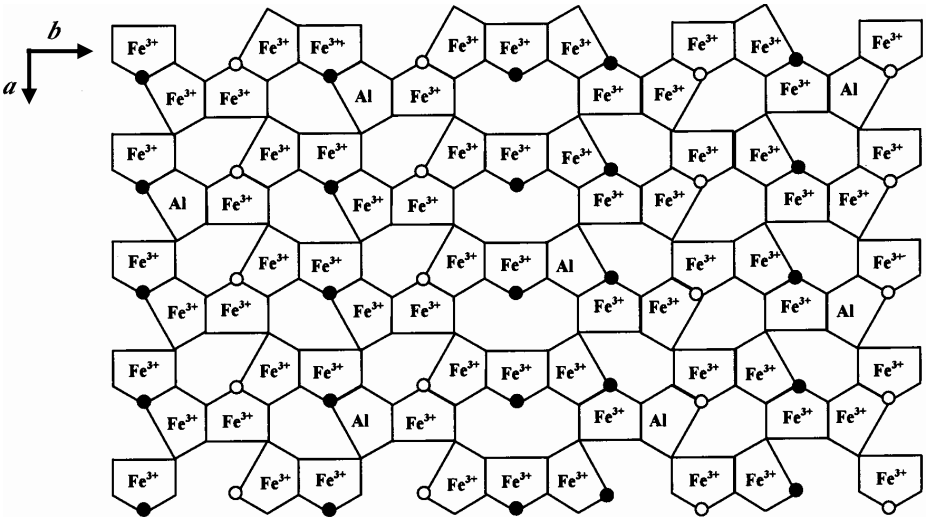

Fig. 5. A portion of the octahedral sheet composed of the two fragments, in which either M21 or M22 sites are vacant. The boundary Fe^{3+}-sites alternate, along the *a* direction, with "holes" formed by two vacant sites merged together.

(Rusakov & Khramov, 1992) shows that nontronite dehydroxylate structure can still be described as a structure having mostly ionic bonds. Second, the atomic coordinates, which were simulated for the 2:1 layer of nontronite-dehydroxylate, proved to be relevant. The validity of the procedure used for structural modeling has thus been confirmed.

The invariability of the EFG parameters calculation with respect to the layer stacking confirms the dominant role of the Fe^{3+} nearest environment in the formation of the EFG at Fe nuclei (Drits *et al.*, 1997; Dainyak *et al.*, 2004). This result justifies the use of atomic coordinates for a periodic crystal structure in the EFG calculations although the actual nontronite dehydroxylate structure may be turbostratic or partially ordered. In addition, this invariability increases the validity of the Fe^{3+}, Fe^{2+} quadrupole doublet assignments to the local cationic arrangements in the octahedral sheets of *trans*-vacant dioctahedral phyllosilicates suggested in the quoted papers.

Nontronite-dehydroxylate may be referred to as a model object, because its structural and compositional peculiarities make it possible to analyze electric field gradients at Fe^{3+} nuclei in five-fold coordination of former *cis*- and *trans*-octahedra using the most straightforward and simple way. The prevalence of the local cationic arrangement [4Si]($3Fe^{3+}$) over [3SiAl]($3Fe^{3+}$) and those including nearest octahedral Al around Fe^{3+} both in former *cis*- and *trans*-octahedra allowed us to use the atomic coordinates for the average structure in the EFG calculations without simulating the atomic coordinates for the above local cationic arrangements.

The presence of the Al cations in octahedral and tetrahedral sheets leads to local inhomogeneity in the dehydroxylate structure displayed in the broadened doublet components Γ, which are approximately three times greater than the apparatus halfwidths equal to 0.21 mm/s (for inner peaks of the α-Fe spectrum), and in the inequality of Γ_{-v} and Γ_{+v} values inside the partial doublets (Table 1, variant 6). Note that such widening may also result from strains and stresses in the dehydroxylated structure.

The obtained assignment adds to our knowledge of the EFG at Fe^{3+} and Fe^{2+} nuclei in *cis*-positions in various local cationic arrangements inherent to *trans*-vacant dioctahedral sheets of micaceous minerals of inhomogeneous composition (Drits *et al.*, 1997; Dainyak *et al.*, 2004). It would be interesting to calculate the EFG at Fe^{3+} nuclei occupying true *cis*- and *trans*- octahdera of their untreated varieties. However, most of such Fe-bearing minerals are *trans*-vacant (Méring & Oberlin, 1967; Besson *et al.*, 1982, 1983; Bonnin *et al.*, 1985; Tsipursky & Drits, 1984; Tsipursky *et al.*, 1978, 1985a; Sakharov *et al.*, 1990; Manceau *et al.*, 2000).

4.1 Defects violating two-dimensional continuity of dehydroxylated octahedral sheets

A structural model for dehydroxylated Fe^{3+}-rich dioctahedral micas determined by Muller *et al.* (1998, 2000) corresponds to an average unit cell in which both symmetrically independent *cis*-sites are partially occupied. These authors emphasized, however, that in the actual structure each dehydroxylated layer consists of structural fragments, in which either M21 or M22 sites are vacant. Figure 5 shows a possible model of the dehydroxylated octahedral sheet composed of two such fragments. These two structural domains are linked through Fe^{3+} in boundary former *trans*-octahedra sharing two edges with nearest former *cis*-octahedra. These boundary Fe^{3+} sites alternate, along the *a* direction, with "holes" formed by two vacant sites merged together. Such structural peculiarities correspond to partial disruption of Fe-O-Fe bonds. Several inferences may follow from this simplified scheme.

1. The boundary former *trans*-octahedra sharing two edges with the nearest former *cis*-octahedra are characterized by extremely high anisotropy in the distribution of USPBS values. The residual O^{2-}_{r} bonded with one Fe^{3+} cation is approximately twice as undersaturated, with respect to positive charge, as a residual O^{2-}_{r} coordinated by two Fe^{3+} cations (Fig. 5). These strongly undersaturated anions may be partially neutralized with interlayer charge. In addition, to improve charge compensation in these unusual polyhedra, the non-shared anion positions may be represented by OH groups, which may have remained in the course of heat-

treatment in order to minimize strongly undersaturated local sources of a negative charge. However, strong deformation of the central Fe^{3+}-polyhedron in these unusual local cationic arrangements should be expected resulting in anomalous Δ values of 2.2 mm/s fitted to the nontronite dehydroxylate spectrum (Table 1).

2. The experimental S_{trans}/S_{cis} ratio is equal to 0.8 (Table 1, variant 6), whereas the expected ratio for the idealized dehydroxylated structure with random cation distribution sheets should be equal to 1. The disruption of the two-dimensional continuity of the dehydroxylated octahedral sheets may be considered as a one of the possible reasons for the observed deviation of the S_{trans}/S_{cis} ratio from the theoretical value. As a matter of fact, unusual boundary positions of Fe^{3+}, adjacent to only two polyhedra (Fig. 5), are former *trans*-octahedra. Therefore the number of former *trans*-octahedra assigned to the doublet with the smaller Δ decreases, leading to a smaller S_{trans}/S_{cis} ratio. This explanation seems to be harmonious from the point of view of the structural model integrity. It should be noted, however, that the QSD and ISD of the minor spectrum components accounting for the local structural inhomogeneity may also affect the S_{trans}/S_{cis} ratio.

3. The holes shown in Fig. 5 extend along the *a* axis and separate the domains with left-hand and right-hand patterns in the distribution of vacant sites and unbroken Fe-O-Fe bonds. Some of these domains may be small enough (< 3–5 nm) to display superparamagnetic properties. From this point of view, the structural model for the dehydroxylated octahedral sheets (Muller *et al*., 1998, 2000) seems to be self-sufficient. However, the formation of superparamagnetic domains, most likely, becomes more prominent in dehydroxylated SWa-1 nontronite (Karakassides *et al*., 2000), which is originally characterized by a specific distribution of diamagnetic cations substituting for Fe^{3+} in octahedral sheets (Manceau *et al.*, 2000). Bearing in mind the appreciable amount of Al cations in octahedral sheets of Garfield nontronite and the lack of Fe^{3+} cations in tetrahedra (Manceau *et al*., 2000), similar superparamagnetic properties may be also expected for Garfield nontronite dehydroxylate under low temperature.

Thus the structural model of dehydroxylated Fe-rich dioctahedral 2:1 phyllosilicates of Muller *et al*. (1998, 2000) accounts for such parameters of the fitted spectrum as the anomalous Δ value of 2.21 mm/s and the S_{trans}/S_{cis} ratio. In addition, superparamagnetic effects expected in low temperature spectra may be explained in terms of this model.

4.2 Isomer shift

One would expect decreasing isomer shifts for the Fe^{3+}-doublets when six-fold coordination transforms into five-fold one. However, these values do not change, which is confirmed by the series of the spectrum refinements (Table 1). This fact deserves a special investigation. As a possible reason, one may speculate, first, that the five-fold polyhedra inherit the shape of the octahedra of the untreated nontronite structure because the residual oxygens are located, with equal probability, in one of the two adjacent former OH positions (Muller *et al.*, 1998, 2000). Second, as it follows from Table 2b, the mean Fe^{3+}-oxygen bond lengths in five-fold polyhedra do not differ dramatically from the mean interatomic distance in the *cis*-octahedra of untreated nontronite (Table 2a). These two points may be a possible reason for the invariable effective density of S electrons and isomer shifts for Fe^{3+} during the dehydroxylation process.

5. Conclusions

EFG calculations in point charge approximation using the modelled atomic coordinates for Garfield nontronite-dehydroxylate provide a reliable interpretation of its Mössbauer spectrum. The doublet with the smallest quadrupole splitting, Δ, is assigned to the former *trans*-octahedra whereas the doublet with the larger Δ value is assigned to the former *cis*-octahedra.

Good agreement between calculated and experimental quadrupole splittings implies that the nontronite-dehydroxylate structure can be described as a structure having mostly ionic bonds.

The invariability of the EFG parameters calculation with respect to the mode in the layer stacking confirms the dominant role of the Fe^{3+} nearest environment in the formation of the EFG at Fe nuclei (Drits *et al.*, 1997; Dainyak *et al.*, 2004).

The structural model of dehydroxylated Fe-rich dioctahedral 2:1 phyllosilicates of Muller *et al*. (1998, 2000) allows disruptions of two-dimensional continuity of dehydroxylated octahedral sheets. This peculiarity accounts for the anomalous Δ value of 2.21 mm/s for Fe^{3+} and the S_{trans}/S_{cis} ratio in the room temperature nontronite dehydroxylate spectrum as well as possible superparamagnetic effects in its low temperature spectra.

Acknowledgments: Authors gratefully acknowledge G.V. Karpova for the microprobe analysis. We wish to thank anonymous reviewers for their valuable comments and suggestions. This research was supported by Russian Foundation for Basic Research (RFFI) (grant 05-05-64135).

References

Bailey, S.W. (1984): Crystal chemistry of the true micas. *in* Micas, Reviews in Mineralogy, S.W. Bailey, ed. Mineralogical Society of America, 13–66.

Besson, G., De La Calle, C., Rautureau, M., Tchoubar, C., Tsipursky, S.I., Drits, V.A. (1982): X-ray and electron diffraction study of the structure of Garfield nontronite. *in* Proc. of VII Intern. Clay Conference, 1981, Italy, H. van Olphen & F. Veniale, eds. Elsevier Sci. Publ., (Amsterdam – Oxford) New York, 29–40.

Besson, G., Bookin, A.S., Dainyak, L.G., Rautureau, M., Tsipursky, S.I., Tchoubar, C., Drits, V.A. (1983): Use of diffraction and Mössbauer methods for the structural and crystallochemical characterization of nontronites. *J. Appl. Cryst.*, **16**, 374–384.

Bonnin, D., Calas, G., Suquet, H., Pezerat, H. (1985): Site occupancy of Fe^{3+} in Garfield nontronite: a spectroscopic study. *Phys. Chem. Minerals*, **12**, 55–64.

Brigatti, M.F. & Guggenheim S. (2002): Mica crystal chemistry and the influence of pressure, temperature and solid solution on atom-

istic models. *in* Reviews in Mineralogy and Geochemistry, 46, Micas: crystal chemistry and metamporphic petrology. A. Mottana, F.E. Sassi, J.B. Thompson Jr. and S. Guggenheim, eds. Mineralogical Society of America with Accademia Nazionale dei Lincei, Roma, Italy, 1–97.

Dainyak, L.G. & Drits, V.A. (1987): Interpretation of Mössbauer spectra of nontronite, celadonite, and glauconite. *Clays Clay Minerals*, **35**, 363–372.

Dainyak, L.G., Drits, V.A., Lindgreen, H. (2004): Computer simulation of octahedral cation distribution and interpretation of the Mössbauer Fe^{2+} components in dioctahedral *trans*-vacant micas. *Eur. J. Mineral.*, **16**, 451–468.

David, W.I.F. (1986): Powder diffraction peak shapes. Parameterization of the pseudo-Voigt as a Voigt function. *J. Appl. Cryst.*, **19**, 63–64.

Drits, V.A., Besson, G., Muller, F. (1995): An improved model for structural transformations of heat- treated aluminous dioctahedral 2:1 layer silicates. *Clays Clay Minerals*, **43**, 718–731.

Drits, V.A., Dainyak, L.G., Muller, F., Besson, G., Manceau, A. (1997): Isomorphous cation distribution in celadonites, glauconites, and Fe-illites determined by infrared, Mössbauer and EXAFS spectroscopies. *Clay Minerals*, **32**, 153–179.

Drits, V.A., McCarty, D.K., Zviagina, B.B. (2006): Crystal-chemical factors responsible for the distribution of octahedral cations over *trans*- and *cis*-sites in dioctahedral 2:1 layer silicates. *Clays Clay Minerals*, **54**, 131–152.

Evans, M.J. & Black, P.J (1970): The Voigt profile of Mössbauer transmission spectra. *J. Phys. C: Solid St. Phys.*, **3**, 2167–2177.

Gates, W.P., Slade, P.G., Manceau, A., Lanson, B. (2002): Site occupancies by iron in nontronites. *Clays Clay Minerals*, **50**, 223–239

Goodman, B.A. (1978): The Mössbauer spectra of nontronites: consideration of an alternative assignment. *Clays Clay Minerals*, **26**, 176–177.

Goodman, B.A., Russel, J.D., Fraser, A.R., Woodhams, F.W.D. (1976): A Mössbauer and I.R. spectroscopic study of the structure of nontronite. *Clays Clay Minerals*, **24**, 53–59.

Heller-Kallai, L. & Rozenson, I. (1980): Dehydroxylation of dioctahedral phyllosilicates. *Clays Clay Minerals*, **28**, 355–368.

Ingalls, R. (1964): Electric-field gradient tensor in ferrous compounds. *Phys. Rev.* **133**, A787–A795.

Karakassides, M.A., Gournis, D., Simopoulos, T., Petridis, D. (2000): Mössbauer and infrared study of heat-treated nontronite. *Clays Clay Minerals*, **48**, 68–74.

Lear, P.R. & Stuki, J.W. (1990): Magnetic properties and site occupancy of iron in nontronite. *Clay Minerals*, **25**, 3–13.

Lin Cheng-yi & Bailey, S.W. (1984): The crystal structure of paragonite $2M_1$. *Am. Mineral.*, **69**, 122–127.

Mamy, J. & Gaultier, J.P. (1976): Les phenomenes de diffraction de rayonnements X et electronique per les reseaux atomiques: application à l'étude de l'ordre dans les mineraux argileux. *Annual Agronomiques*, **27**, 1–16.

Manceau, A., Ghateigner, D., Gates, W.P. (1998): Polarized EXAFS, distance-valence least-squares modeling (DVLS), and quantitative texture analysis approaches to the structural refinement of Garfield nontronite. *Phys. Chem. Minerals*, **25**, 347–365.

Manceau, A., Lanson, B., Drits, V.A., Chateigner, D., Gates, W.P., Wu, J., Huo, D., Stuki, J.W. (2000): Oxidation-reduction mechanism of iron in dioctahedral smectites. I. Crystal chemistry of oxidized reference nontronites. *Am. Mineral.*, **85**, 133–152.

Martin, P. & Puerta, J. (1981): Three and four generalized Lorentzian approximations for the Voigt line shape. *Applied Optics*, **20**, 3923–3928.

Méring, J. & Oberlin, A. (1967): Electron-optical study of smectites. *Clays Clay Minerals*, **15**, 3–25.

Muller, F., Plancon, A., Drits, V.A., Besson, G. (1998): Modelisation of X-ray powder diffraction patterns for the study of heat-treated Fe-rich dioctahedral 2:1 layer silicates. *J. Phys. IV*, **8**, 91–98.

Muller, F., Drits, V.A., Plancon, A., Besson, G. (2000): Dehydroxylation of Fe^{3+}, Mg-rich dioctahedral micas: (I) structural transformation. *Clay Minerals*, **35**, 491–504.

Popov, V.I., Khramov, D.A., Lobanov, F.I. (1988): Absorber shape: The influence on the Mössbauer spectra parameters. *in* Proc. of USSR conference on applied Mössbauer spectroscopy "Volga", Moscow Physical Engineering Inst., Moscow, 32–33 (in Russian).

Presniakov I., Baranov A., Demazeau G., Rusakov V., Alonso J., Sobolev A., Pokholok K. (2006): Evidence through Mössbauer spectroscopy of two different states for ^{57}Fe probe atoms in $RNiO_3$ perovskites with intermediate-size rare earths, R = Sm, Eu, Gd, Dy. *Phys. Rev. B.* (accepted for publication).

Rancourt, D.G. & Ping, J.Y. (1991): Voigt-based methods for arbitrary-shape static hyperfine parameter distribution in Mössbauer spectroscopy. *Nucl. Instrum Methods Phys. Res.*, **B58**, 85–97.

Rusakov, V.S. (1999): Reconstruction of the hyperfine parameters distributions for Mössbauer spectra of locally inhomogeneous systems. *Bul. Russ. Acad. Sci. Phys.*, **7**, 1093–1098.

– (2000): Methods to deriving information from Mössbauer spectra of locally inhomogeneous systems (Complex MS Tools). *in* "Mössbauer spectroscopy of locally inhomogeneous systems", Alma-Ata, 11–86 (in Russian).

– (2005): Physical principles of Mössbauer spectroscopy. Part II. Experiment. Moscow State University, Moscow, 30 p. (in Russian).

Rusakov, V.S. & Chistyakova, N.I. (1992): Mössbauer Program Complex MSTools. Latin American conference on applications of the Mössbauer effect, LACAME'92. Abstracs. Buenos Aires. Argentina, 7, 3.

Rusakov, V.S. & Khramov, D.A. (1992): The problem of choice ^{57}Fe nucleus quadrupole moment value in Mössbauer spectroscopy. *Bull. Russ. Acad. Sci. Phys.*, V.**56**, " 7, 1118–1120.

Sakharov, B.A., Besson, G., Drits, V.A., Kameneva, M.Yu., Salyn, A.L., Smoliar, B.B. (1990): X-ray study of the nature of stacking faults in the structure of glauconites. *Clay Minerals*, **25**, 419–435.

Semenova, T.F., Rozhdestvenskaya, I.V., Frank-Kamenetskii, V.A. (1977): Refinement of the crystal structure of tetraferriphlogopite, *Sov. Phys. Crystallogr.*, **22**, 680–683.

Sherman, D.M. & Vergo, N. (1988): Optical (diffuse reflectance) and Mössbauer spectroscopic study of nontronite and related Fe-bearing smectites. *Am. Mineral.*, **73**, 1346–1354.

Smoliar-Zviagina, B.B. (1993): Relationship between structural parameters and chemical composition of micas. *Clay Minerals*, **28**, 603–624.

Sternheimer, R.M. (1963): Quadrupole antishielding factors of ions. *Phys. Rev.*, **130**, 1423–1425.

Tsipursky, S.I. & Drits, V.A. (1984): The distribution of octahedral cations in the 2:1 layers of dioctahedral smectites studied by oblique-texture electron diffraction. *Clay Minerals*, **19**, 177–193.

Tsipursky, S.I., Drits, V.A., Chekin, S.S. (1978): Revealing of the structure ordering of nontronites by oblique texture electron diffraction. *Izvesiya Akademii Nauk S.S.S.R.,Seriya Geologicheskaya*, **10**, 105–113 (in Russian).

Tsipursky, S.I., Drits, V.A., Plancon, A. (1985a): Calculation of the intensities distribution in oblique texture electron diffraction patterns. *Sov. Phys. Crystallogr.*, **30**, 38–44.

Tsipursky, S.I., Kameneva, M.Yu., Drits, V.A. (1985b): Structural transformations of Fe^{3+} –containing 2:1 dioctahedral pyllosilica-

tes in the course of dehydration. *in* Proc. 5th Meeting of the European Clay Group, Prague, 1983, J. Konta ed. Charles University, Prague, 1985, 569–577.

Udagava, S., Urabe, K., Hasu, H. (1974): The crystal structure of muscovite dehydroxylate. *Jap. Assoc. Mineral. Petrol. Econom. Geo*. **69**, 381–389.

Wardle, R. & Brindley, G.W. (1972): The crystal structures of pyrophyllite-1Tc and its dehydroxylate. *Am. Mineral.*, **57**, 732–750.

Received 17 October 2005
Modified version received 18 May 2006
Accepted 10 July 2006